Eur. Phys. J. Plus (2021) 136:507
https://doi.org/10.1140/epjp/s13360-021-01509-6

THE EUROPEAN PHYSICAL JOURNAL PLUS

Regular Article

Angular deviations: from a cubic equation to a universal closed formula to determine the peak position of reflected and (upper) transmitted beams

Stefano De Leo[1,a], **Alessia Stefano**[2]

[1] Department of Applied Mathematics, State University of Campinas, São Paulo, Brazil
[2] Department of Mathematics and Physics, University of Salento, Lecce, Italy

Received: 9 March 2021 / Accepted: 27 April 2021

Abstract Angular deviations and lateral displacements are optical effects widely investigated in the literature. In this paper, by using the Taylor expansion of the Fresnel coefficients, we obtain an analytic expression for the beam reflected by and (upper) transmitted through a dielectric prism. These analytical approximations lead to a cubic equation which allows to determine the angular deviations of the optical beams. Near the Brewster angles, under specific conditions, we obtain a universal formulation for the cubic equation. Its explicit solution determines the peak position of the reflected and (upper) transmitted beams. The universal solution could be of great utility in future experimental implementations. The analytic results show an excellent agreement with the numerical calculation, and the analytic expressions given for the reflected and (upper) transmitted beams should play an important role in the weak measurements analysis.

1 Introduction

The optical path of a Gaussian beam reflected by or transmitted trough a dielectric prism can easily be calculated by using the laws of geometric optics [1,2]. As the reflection and Snell laws surely represent a useful tool to describe the propagation of optical beams, they cannot be used to predict or explain phenomena like lateral displacements [3–22] and/or angular deviations [23–34].

Lateral displacements, known as Goos-Hänchen shifts in honour of the German researchers that in 1947 realized, for transverse electric waves, the first experiment of this phenomenon [3], can theoretically be explained by using the stationary phase method as done by Artmann in 1948 [4]. The additional phase, which characterizes the Fresnel coefficients in the case of total reflection, is indeed responsible for the lateral displacement. The Artmann formula provides an accurate estimate of the lateral displacement in terms of the light wavelength, refractive index, and incidence angle. It is polarization dependent and, consequently, implies different lateral shifts for transverse electric and magnetic waves. After the Artmann work, the German researchers tested the theoretical Artmann prediction by repeating the experiment for transverse magnetic waves [7]. Due to the fact that the shifts are proportional

[a] e-mail: deleo@unicamp.br (corresponding author)

Published online: 07 May 2021

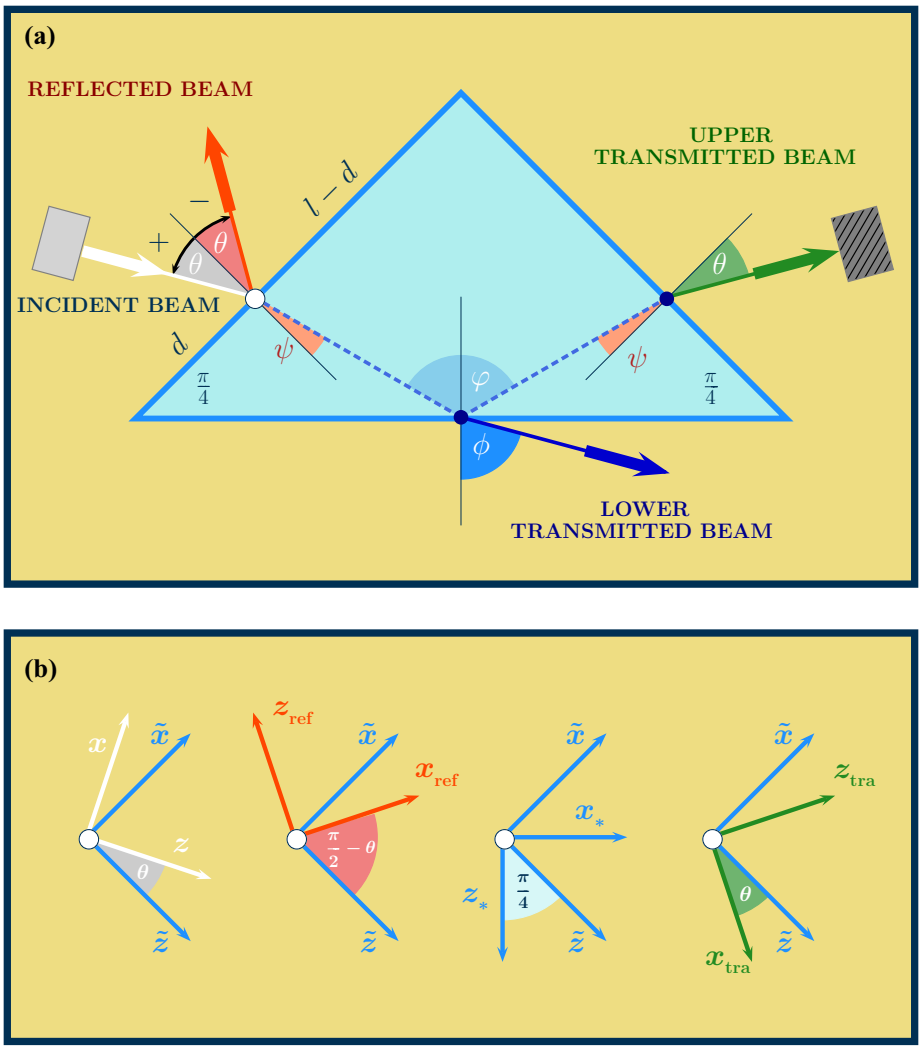

Fig. 1 The optical system used in this paper and the coordinate systems of the incident, the lower and upper transmitted beams. The $\widetilde{z}$ and $\widetilde{x}$ axes are, respectively, the normals to the incident air/dielectric interface and the upper dielectric/air interface. The z_* axis is the normal to the lower dielectric/air interface. The angles ψ, φ, and ϕ contain an implicit dependence on the incidence angle θ and the refractive index n: $\sin\theta = n\ \sin\psi$, $\varphi = \psi + \pi/4$, and $n\ \sin\varphi = \sin\phi$

to the beam wavelength, Goos and Hänchen used an elongated dielectric block to amplify the effect. For an optical beam transmitted through a dielectric prism, lateral displacements appear in the upper transmitted beam when the angle, θ, that the incident beam forms with the first air/dielectric interface is greater than the critical angle, $\varphi_{\text{cri}} = \arcsin(1/n)$, see Fig. 1. In this case, it is common to use weak measurements to amplify the lateral displacements [17,21]. In the region of *pure* total reflection, the prediction of the Artmann formula was widely confirmed in the experiments [17,18,21,22]. Nevertheless, for incidence at critical angle, the Artmann lateral displacement tends to infinity and numerical calculations are

needed to reproduce the experimental data. In 1971 [10], Horowitz and Tamir, by using a Fresnel approximation in the Gaussian integral form of the optical beam, derived the lateral displacement for angles of incidence that are arbitrarily close to the critical one. They proposed a formula in terms of parabolic-cylinder (Weber) functions which reproduced the classical one for large beam widths and for incidence angles that are not too close to the critical angle. As the incidence angle approaches the critical angle, the beam shift approaches a constant value that is dependent on the beam width [10,19]. They also found that the maximum lateral displacement occurred at an angle that is slightly larger than the critical one. In 2016 [20], a closed formula in terms of modified Bessel functions of the first kind was obtained by studying the angular distribution of the optical beam. The new formula allowed to understand how the breaking of symmetry in the angular distribution causes a difference between experimental measurements done by calculating the maximum and the mean value of the beam intensity. This study also showed the lateral displacement dependence on the angular distribution shape of the incoming beam. The theoretical prediction was confirmed by the experiments described in [21,22].

As described before, for *pure* total reflection, the additional phase which appears in the Fresnel coefficients is responsible for lateral displacements. In the case of *pure* partial reflection, the Fresnel coefficients are real, so the optical beam does not present any lateral shifts. Nevertheless, the breaking of symmetry in the Fresnel coefficients generates angular deviations. In 1985 [25], Chan and Tamir analysed the angular deviation in the region around the Brewster angle. They used a mathematical method similar to the one of ref. [10] offering an interesting presentation of the phenomenon near the Brewster angle, where the reflected beam, as we shall see explicitly later, is so deformed in comparison with the incident one that the concept of angular deviation lacks any meaning. Few years later [26], the authors also discussed the angular deviations near the critical angle reviewing previous works [23,24]. In 2009 [30,31], Aiello and Woerdman revisited the topic of angular deviations in the Brewster region [27], calculating the mean value of the angular deviations from geometric optics. A closed form expression for angular deviations of the Snell law in the case of maximal symmetry breaking at critical angle was obtained in [33]. As it is happens for lateral displacements, the weak measurement technique can be used to amplify such deviations [34]. The reader can find a tutorial review of lateral shifts and angular deviations of Gaussian beams in [35]. It is important to observe that for an optical beam reflect by and transmitted through a dielectric prism, we have *three* Brewster angles: Two for the reflected beam, $\theta_{\text{exB}} = \pm \arctan[n]$, and one for the upper transmitted one, $\varphi_{\text{inB}} = \arctan[1/n]$, see Fig. 1.

For incidence near the critical angle, under certain conditions, angular deviations and lateral displacement act simultaneously generating the effect of axial dependence of the Goos-Hänchen shift and the oscillatory behaviour of light [36]. This intriguing phenomenon was recently confirmed experimentally [37,38].

The subject matter of our investigation is the study of angular deviations in the Brewster regions for the optical beams reflected by and transmitted through a dielectric prism and in the critical region for the (upper) transmitted beam. The paper is structured as follows. Section 2 introduces the formalism, the free Gaussian beam, the optical system, and the Fresnel coefficients. Section 3 contains the analytical approximation of the reflected beam from which we obtain the cubic equation for the peak. In this Section, for incidence near the external Brewster angles and for an axial distance greater than the Rayleigh radius, we obtain, for the angular deviations, a universal formula to determine the peak of the beam. This allows to compare the mean value and maximum analysis of angular deviations. The analytical predictions show an excellent agreement with numerical calculation. In Section

4, we discuss the (upper) transmitted beam and the amplification near the internal Brewster angle and the critical one. Conclusions and further investigations appear in the last Section.

2 Spatial optical phases

The propagation of a Gaussian beam which moves from the source to the left air/dielectric interface of a dielectric prism, see Fig. 1, is described by the following integral

$$E^{[\mathrm{inc}]}(x,y,z) = E_0 \int \mathrm{d}k_x \int \mathrm{d}k_y \; G(k_x,k_y) \times \exp\left[\, i\,(k_x x + k_y y + k_z z)\,\right], \tag{1}$$

where

$$G(k_x,k_y) = \mathrm{w}_0^2 \exp\left[-\left(k_x^2+k_y^2\right)\mathrm{w}_0^2/4\right]/4\pi,$$

is the Gaussian wave number distribution, w_0 is the waist radius, and

$$k_z = \sqrt{k^2-k_x^2-k_y^2} \;\approx\; k-(k_x^2+k_y^2)/2k$$

is a function of k_x and k_y and contains the wavelength λ ($k=2\pi/\lambda$). By using the previous approximation, valid for $\mathrm{w}_0 \geq \lambda$, the integral in Eq. (1) can be analytically solved

$$E^{[\mathrm{inc}]}(x,y,z) = \frac{E_0\, e^{ikz}}{1+i\,z/z_R} \exp\left[-\frac{x^2+y^2}{\mathrm{w}_0^2\,(1+i\,z/z_R)}\right] \tag{2}$$

where $z_R = k\,\mathrm{w}_0^2/2$ is the Rayleigh length. The intensity of the incident beam is then given by

$$I^{[\mathrm{inc}]}(x,y,z) = I_0 \frac{\mathrm{w}_0^2}{\mathrm{w}^2(z)} \exp\left[-2\,\frac{x^2+y^2}{\mathrm{w}^2(z)}\right] \tag{3}$$

where $I_0 = |E_0|^2$ and $\mathrm{w}(z) = \mathrm{w}_0\sqrt{1+(z/z_R)^2}$ is the radius at which the field intensity falls to $1/e^2$.

In order to obtain the integral form of the reflected and (upper) transmitted beam, we first calculate the respective spatial optical phases. This will be done by introducing the appropriate coordinate systems, see Fig. 1. For the left (air/dielectric) interface and the right (dielectric/air) one, we have the $(\widetilde{x},\widetilde{z})$ system, for the lower (dielectric/air interface) the (x_*, z_*) system, and, finally, for the reflected and (upper) transmitted beam we, respectively, have the $(x_{\mathrm{ref}}, z_{\mathrm{ref}})$ and $(x_{\mathrm{tra}}, z_{\mathrm{tra}})$ coordinates.

By a θ rotation, the spatial phase of the incident beam can be rewritten in terms of the left (air/dielectric) interface system as follows

$$k_x\,x + k_y\,y + k_z\,z = k_{\tilde{x}}\,\widetilde{x} + k_y\,y + k_{\tilde{z}}\,\widetilde{z}.$$

The spatial phase of the reflected beam is then given by

$$k_{\tilde{x}}\,\widetilde{x} + k_y\,y - k_{\tilde{z}}\,\widetilde{z}.$$

By using the matrix algebra, we can rewrite

$$\left(k_{\tilde{x}} \quad k_{\tilde{z}}\right)\begin{pmatrix}\widetilde{x}\\ -\widetilde{z}\end{pmatrix},$$

in terms of k_x, k_y, and the proper coordinate system of the reflected beam

$$\begin{aligned}&\begin{pmatrix} k_x & k_z \end{pmatrix} \begin{pmatrix} \cos\theta & -\sin\theta \\ \sin\theta & \cos\theta \end{pmatrix} \begin{pmatrix} 1 & 0 \\ 0 & -1 \end{pmatrix} \\ &\quad \times \begin{pmatrix} \sin\theta\ \cos\theta \\ -\cos\theta\ \sin\theta \end{pmatrix} \begin{pmatrix} z_{\text{ref}} \\ x_{\text{ref}} \end{pmatrix} \\ &\quad = \begin{pmatrix} k_x & k_z \end{pmatrix} \begin{pmatrix} x_{\text{ref}} \\ z_{\text{ref}} \end{pmatrix} \qquad .\end{aligned}$$

The integral form of the reflected beam,

$$\begin{aligned}E^{[\text{ref}]}_{\text{pol}}(x_{\text{ref}}, y, z_{\text{ref}}) = E_0 \int \mathrm{d}k_x \int \mathrm{d}k_y\ G^{[\text{ref}]}_{\text{pol}}(k_x, k_y) \\ \times \exp\left[\, i\, (k_x\, x_{\text{ref}} + k_y\, y + k_z\, z_{\text{ref}})\, \right],\end{aligned} \tag{4}$$

is polarization dependent. This is due to the fact that the wave number distribution,

$$G^{[\text{ref}]}_{\text{pol}}(k_x, k_y) = R_{\text{pol}}(k_x, k_y)\, G(k_x, k_y),$$

contains the Fresnel coefficients

$$R_{\text{pol}}(k_x, k_y) = \frac{a_{\text{pol}} k_{\tilde{z}} - q_{\tilde{z}}/a_{\text{pol}}}{a_{\text{pol}} k_{\tilde{z}} + q_{\tilde{z}}/a_{\text{pol}}},$$

where

$$\left\{ a_{\text{te}}\ ,\ a_{\text{tm}} \right\} = \{\, 1\ ,\ n\,\},$$

with the subscript which indicate transverse electric (te) and magnetic (tm) waves.

The spatial phase of the transmitted beam at the left (air/dielectric) interface is given by

$$q_{\tilde{x}}\, \widetilde{x} + k_y\, y + q_{\tilde{z}}\, \widetilde{z},$$

where

$$q_{\tilde{x}} = k_{\tilde{x}} \quad \text{and} \quad q_{\tilde{z}} = \sqrt{n^2 k^2 - q_{\tilde{x}}^2 - k_y^2}$$

In terms of the coordinates system of the lower (dielectric/air) interface, the previous phase can be rewritten as

$$q_{x_*}\, x_* + k_y\, y + q_{z_*}\, z_*$$

which, after reflection at the lower (dielectric/air) interface, becomes

$$q_{x_*}\, x_* + k_y\, y - q_{z_*}\, z_*.$$

As done for the reflected beam, by using the matrix algebra, we find

$$\begin{aligned}&\begin{pmatrix} q_{x_*} & q_{z_*} \end{pmatrix} \begin{pmatrix} x_* \\ -z_* \end{pmatrix} \\ &\quad = \frac{1}{\sqrt{2}} \begin{pmatrix} q_{\tilde{x}} & q_{\tilde{z}} \end{pmatrix} \begin{pmatrix} 1 & -1 \\ 1 & 1 \end{pmatrix} \begin{pmatrix} 1 & 0 \\ 0 & -1 \end{pmatrix}\end{aligned}$$

$$\times \frac{1}{\sqrt{2}} \begin{pmatrix} 1 & 1 \\ -1 & 1 \end{pmatrix} \begin{pmatrix} \widetilde{x} \\ \widetilde{z} \end{pmatrix}$$
$$= \begin{pmatrix} q_{\widetilde{x}} & q_{\widetilde{z}} \end{pmatrix} \begin{pmatrix} \widetilde{z} \\ \widetilde{x} \end{pmatrix}.$$

From this spatial phase, observing that $q_{\widetilde{x}} = k_{\widetilde{x}}$ and that the normal to the right (dielectric/air) interface is $\widetilde{x}$, we immediately obtain the one of the transmitted beam

$$k_{\widetilde{x}}\,\widetilde{z} + k_y\,y + k_{\widetilde{z}}\,\widetilde{x}.$$

This phase can be rewritten in terms of k_x, k_y, and the proper system of the (upper) transmitted beam

$$\begin{pmatrix} k_x & k_z \end{pmatrix} \begin{pmatrix} \cos\theta & -\sin\theta \\ \sin\theta & \cos\theta \end{pmatrix} \begin{pmatrix} 0 & 1 \\ 1 & 0 \end{pmatrix}$$
$$\times \begin{pmatrix} \cos\theta & -\sin\theta \\ \sin\theta & \cos\theta \end{pmatrix} \begin{pmatrix} z_{\text{tra}} \\ x_{\text{tra}} \end{pmatrix}$$
$$= \begin{pmatrix} k_x & k_z \end{pmatrix} \begin{pmatrix} x_{\text{tra}} \\ z_{\text{tra}} \end{pmatrix}.$$

Finally,

$$E^{[\text{tra}]}_{\text{pol}}(x_{\text{tra}}, y, z_{\text{tra}}) = E_0 \int \mathrm{d}k_x \int \mathrm{d}k_y\; G^{[\text{tra}]}_{\text{pol}}(k_x, k_y) \times \exp\left[\, i\,(k_x\,x_{\text{tra}} + k_y\,y + k_z\,z_{\text{tra}})\,\right] \tag{5}$$

where

$$G^{[\text{tra}]}_{\text{pol}}(k_x, k_y) = T_{\text{pol}}(k_x, k_y)\,G(k_x, k_y)$$

and

$$T_{\text{pol}}(k_x, k_y) = \frac{4\,k_{\widetilde{z}}\,q_{\widetilde{z}}}{\left(a_{\text{pol}}\,k_{\widetilde{z}} + q_{\widetilde{z}}/a_{\text{pol}}\right)^2} \frac{q_{z*}/a_{\text{pol}} - a_{\text{pol}}\,k_{\widetilde{z}}}{q_{z*}/a_{\text{pol}} + a_{\text{pol}}\,k_{z*}} \times \exp\{\, i\,[\,q_{z*}\,d\,\sqrt{2} + (q_{\widetilde{z}} - k_{z*})\,(\ell - d)\,]\,\}.$$

The phase which appears in the Fresnel coefficients is due to the fact that the lower and right (dielectric/air) interfaces do not coincide with the origin of the coordinate systems which we have fixed to the left (air/dielectric) interface. Experimentally, this means that the minimal waist is found at such an interface. Such a phase is responsible for the optical geometrical path predicted by the Snell's law [39].

Numerical integrations of Eqs. (4) and (5) can be used to study the propagation of the reflected and (upper) transmitted beam. In particular, to analyse angular deviations and lateral displacements. Nevertheless, analytical approximations for the optical beams are important to understand the physical parameters which characterize such phenomena and to determine the best experimental configuration to observe angular deviations and lateral displacements. In this spirit, in next sections, we look for analytic expressions of the reflected and (upper) transmitted beams. Such approximations, once tested by the numerical calculations, are then used to obtain a cubic equation from which it is possible to determine the angular deviations of the optical beams.

3 The reflected beam

In order to obtain an analytic expression for the reflected beam, we consider the first-order Taylor expansion of the reflection coefficient, i.e.

$$R_{\rm pol}(k_x, k_x) \;=\; R_{\rm pol}(0,0)\,\big[\,1 \,+\, \alpha_{\rm pol}\,k_x/k\,\big], \tag{6}$$

where

$$R_{\rm pol}(0,0) = \frac{a_{\rm pol}\cos\theta - n\cos\psi/a_{\rm pol}}{a_{\rm pol}\cos\theta + n\cos\psi/a_{\rm pol}}$$

and

$$\begin{aligned}\alpha_{\rm te} &= 2\,\tan\psi,\\ \alpha_{\rm tm} &= 2\,\tan\psi\,/\,(\sin^2\psi \,-\, \cos^2\theta).\end{aligned}$$

Observing that the k_x dependence in (6) can be substituted by $-\,i\,\partial_x$ in the integrand of the reflected beam, Eq. (4) becomes analytically solvable. The electric field of the reflected beam is then approximated by

$$\begin{aligned}E^{[\rm ref]}_{\rm pol}(x_{\rm ref}, y, z_{\rm ref}) = &\left[1 + i\;\frac{\alpha_{\rm pol}x_{\rm ref} + z_{\rm ref}}{z_R}\right]\\ &\times\frac{R_{\rm pol}(0,0)}{1 + i\,z_{\rm ref}/z_R}\;E^{[\rm inc]}(x_{\rm ref}, y, z_{\rm ref}).\end{aligned} \tag{7}$$

Consequently, we find the following analytical expression for the field intensity

$$\begin{aligned}I^{[\rm ref]}_{\rm pol}(x_{\rm ref}, y, z_{\rm ref}) = &\left[1 + \left(\frac{\alpha_{\rm pol}x_{\rm ref} + z_{\rm ref}}{z_R}\right)^2\right]\\ &\times\frac{\mathrm{w}_0^2}{\mathrm{w}^2(z_{\rm ref})}\;R^2_{\rm pol}(0,0)\;I^{[\rm inc]}(x_{\rm ref}, y, z_{\rm ref}).\end{aligned} \tag{8}$$

This analytical approximation is checked by numerical calculations. The plots in Fig. 2, done for different incidence angles, $\theta_{\rm exB} + \delta\,/\,k\mathrm{w}_0$, and axial distances, show an excellent agreement between analytic curves and numeric data.

3.1 The external Brewster angle

As observed in the Introduction, we have to differentiate between the Brewster angles of the transverse magnetic waves at the left (air/dielectric) and lower (dielectric/air) interfaces. So, we introduce the terminology of *external* and *internal* Brewster angles. The external Brewster angle refers to the reflection at the left (air/dielectric) interface, and it is determined by $n\,\cos\theta = \cos\psi$. After simple algebraic manipulation, we find

$$\tan\theta_{\rm exB} = \pm\,n. \tag{9}$$

For incidence at Brewster angle, the field is given by

$$\begin{aligned}I^{[\rm ref]}_{\rm exB}(x_{\rm ref}, y, z_{\rm ref}) = &\left[f(n)\;\frac{x_{\rm ref}}{z_R}\,\frac{\mathrm{w}_0}{\mathrm{w}(z_{\rm ref})}\right]^2\\ &\times I^{[\rm inc]}(x_{\rm ref}, y, z_{\rm ref}),\end{aligned} \tag{10}$$

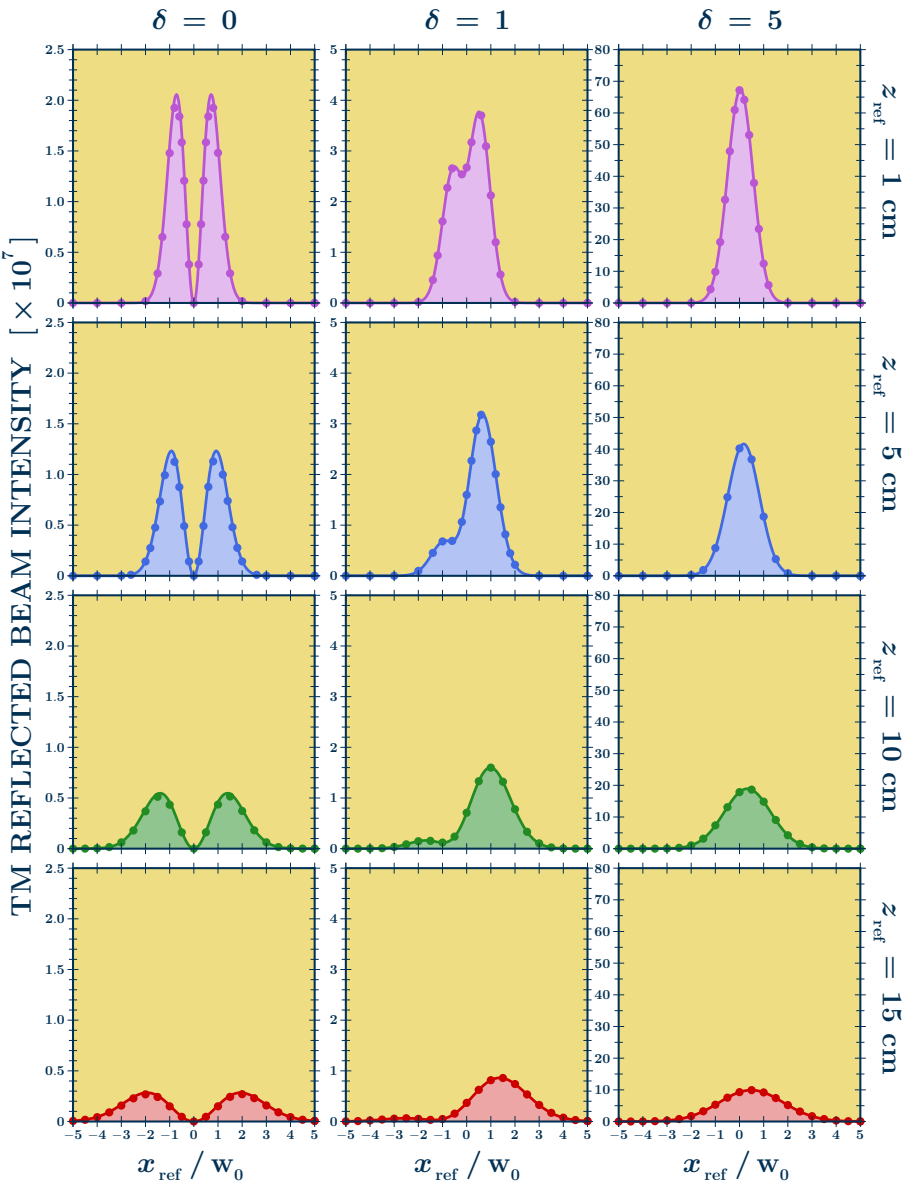

Fig. 2 Field intensity profiles of the reflected beam, $I_{\mathrm{tm}}^{[\mathrm{ref}]}(x_{\mathrm{ref}}, 0, z_{\mathrm{ref}})/I_0$, obtained for an incident Gaussian laser with $\mathrm{w}_0 = 100\,\mu\mathrm{m}$ and $\lambda = 532\,\mathrm{nm}$. The plots refer to different incidence angles, $\theta_{\mathrm{exB}} + \delta\,/\,k\mathrm{w}_0$, and axial distances and a BK7 prism ($n = 1.5195$). The analytic curves (continuous lines) and numeric data (plots) show an excellent agreement. At the Brewster angle, we find the phenomenon of the double peak intensity. For the laser parameters used, the incidence $\delta = 1$ corresponds to $\theta_{\mathrm{exB}} + 0.05°$

where

$$f(n) = \lim_{\theta \to \theta_{\text{exB}}} \alpha_{\text{tm}} R_{\text{tm}}(0,0)$$
$$= \pm \frac{\sqrt{1+n^2}}{n^2} \lim_{\theta \to \theta_{\text{exB}}} \frac{n\cos\theta - \cos\psi}{\sin^2\psi - \cos^2\theta} = \pm \frac{1-n^4}{2n^3}.$$

The reflection coefficient R_{tm} is zero, but it is compensated by the zero in the denominator of α_{tm}. From (10), we immediately calculate the position of the double peaks in the field intensity

$$x_{\text{ref}}^{[\max]} = \pm\, \text{w}(z_{\text{ref}})/\sqrt{2}.$$

For a Gaussian beam with $\text{w}_0 = 100\,\mu\text{m}$ and $\lambda = 532\,\text{nm}$, the Rayleigh range is 5.9 cm. Consequently, at the axial distances 1, 5, 10, and 15 cm, we find

$$x_{\text{ref}}^{[\max]}/\text{w}_0 = \pm\{0.72,\ 0.93,\ 1.39,\ 1.93\},$$

see Fig. 2 for $\delta = 0$. The maxima of the field intensity are

$$\left[\frac{f(n)}{\sqrt{2}\pi}\,\frac{\lambda}{\text{w}_0}\right]^2 \times \exp[-1] \times \left[\frac{\text{w}_0}{\text{w}(z_{\text{ref}})}\right]^2.$$

For the Gaussian beam considered in this paper, we obtain the following reduction factor

$$\left[\frac{f(1.5195)}{\sqrt{2}\pi}\,\frac{0.532}{100}\right]^2 \times \frac{1}{e} \approx 2 \times 10^{-7}$$

with respect to the intensity of the incident beam. The plots of Fig. 2 show that by increasing δ we recover the symmetry of the incident beam, and this allows to use the mean value calculation to estimate the angular deviations.

3.2 The mean value calculation

For a symmetric beam mean and maximum coincide, so the angular deviations can be calculated by using

$$\langle x_{\text{ref}} \rangle_{\text{pol}} = \frac{\int \text{d}x_{\text{ref}} \int \text{d}y\ x_{\text{ref}}\, I_{\text{pol}}^{[\text{ref}]}(x_{\text{ref}}, y, z_{\text{ref}})}{\int \text{d}x_{\text{ref}} \int \text{d}y\ I_{\text{pol}}^{[\text{ref}]}(x_{\text{ref}}, y, z_{\text{ref}})}. \tag{11}$$

Observing that the intensity exponential is an even function in the transversal components, the x_{ref} linear term in Eq. (8) is the only contribution to the numerator, whereas the constant and quadratic terms are the ones which contribute to the denominator,

$$\langle x_{\text{ref}} \rangle_{\text{pol}} = \frac{2\,\frac{\alpha_{\text{pol}}\, z_{\text{ref}}}{z_R^2} \int \text{d}x_{\text{ref}} \int \text{d}y\ x_{\text{ref}}^2\, I^{[\text{inc}]}(x_{\text{ref}}, y, z_{\text{ref}})}{\int \text{d}x_{\text{ref}} \int \text{d}y \left[\frac{\text{w}^2(z_{\text{ref}})}{\text{w}_0^2} + \frac{\alpha_{\text{pol}}^2 x_{\text{ref}}^2}{z_R^2}\right] I^{[\text{inc}]}(x_{\text{ref}}, y, z_{\text{ref}})}. \tag{12}$$

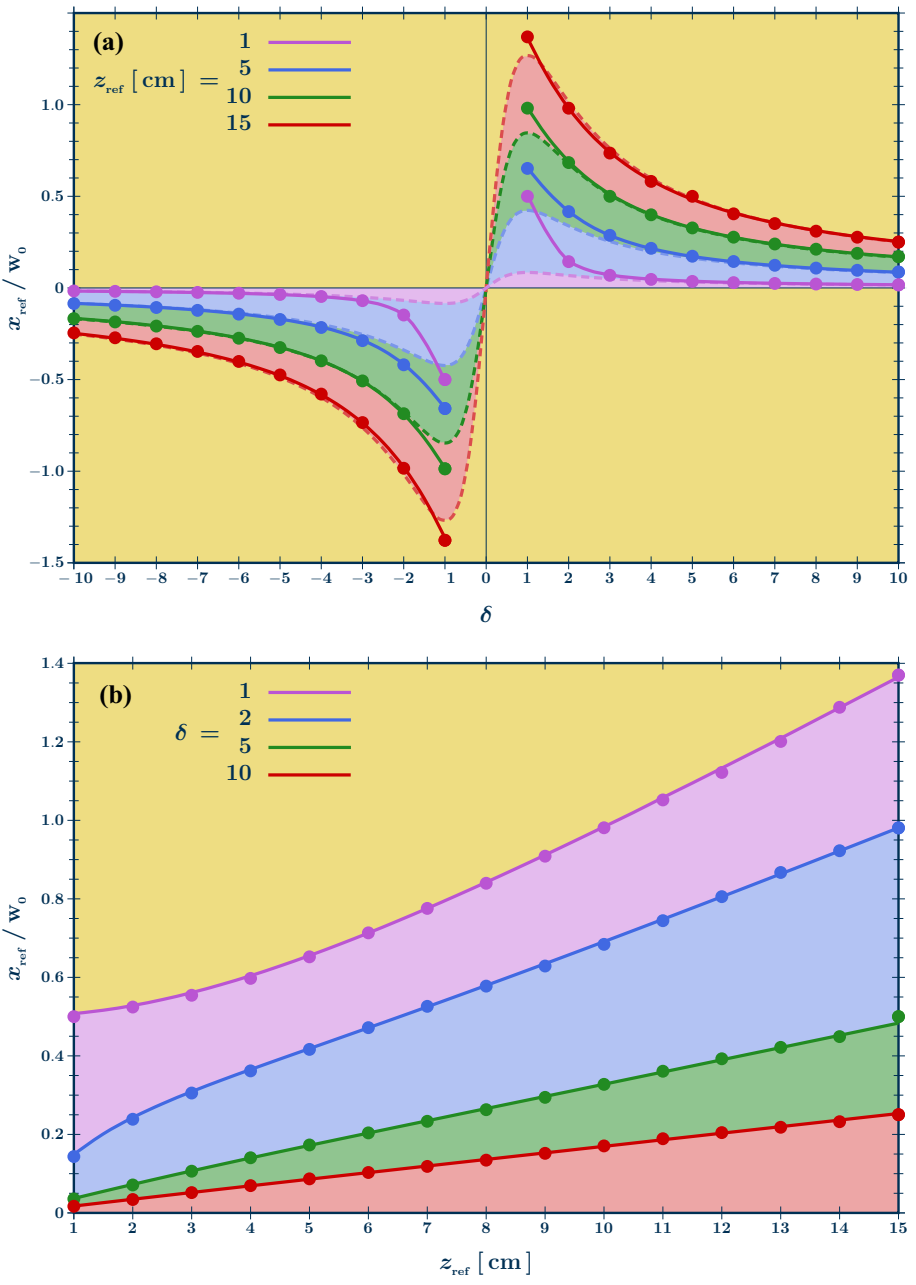

Fig. 3 The solutions of the cubic equation for transverse magnetic waves and incidence near the Brewster angle (continuous lines) are plotted as a function of δ for different values of z_{ref} (upper plots) and as a function of z_{ref} for different values of δ (lower plots). The mean value calculation and numerical data, respectively, appear as dashed lines and dots. The beam parameters are $w = 100\,\mu$m and $\lambda = 0.532$ nm and the refractive index $n = 1.5195$. The breaking of symmetry is evident when we approach the external Brewster angle and decrease the axial distance

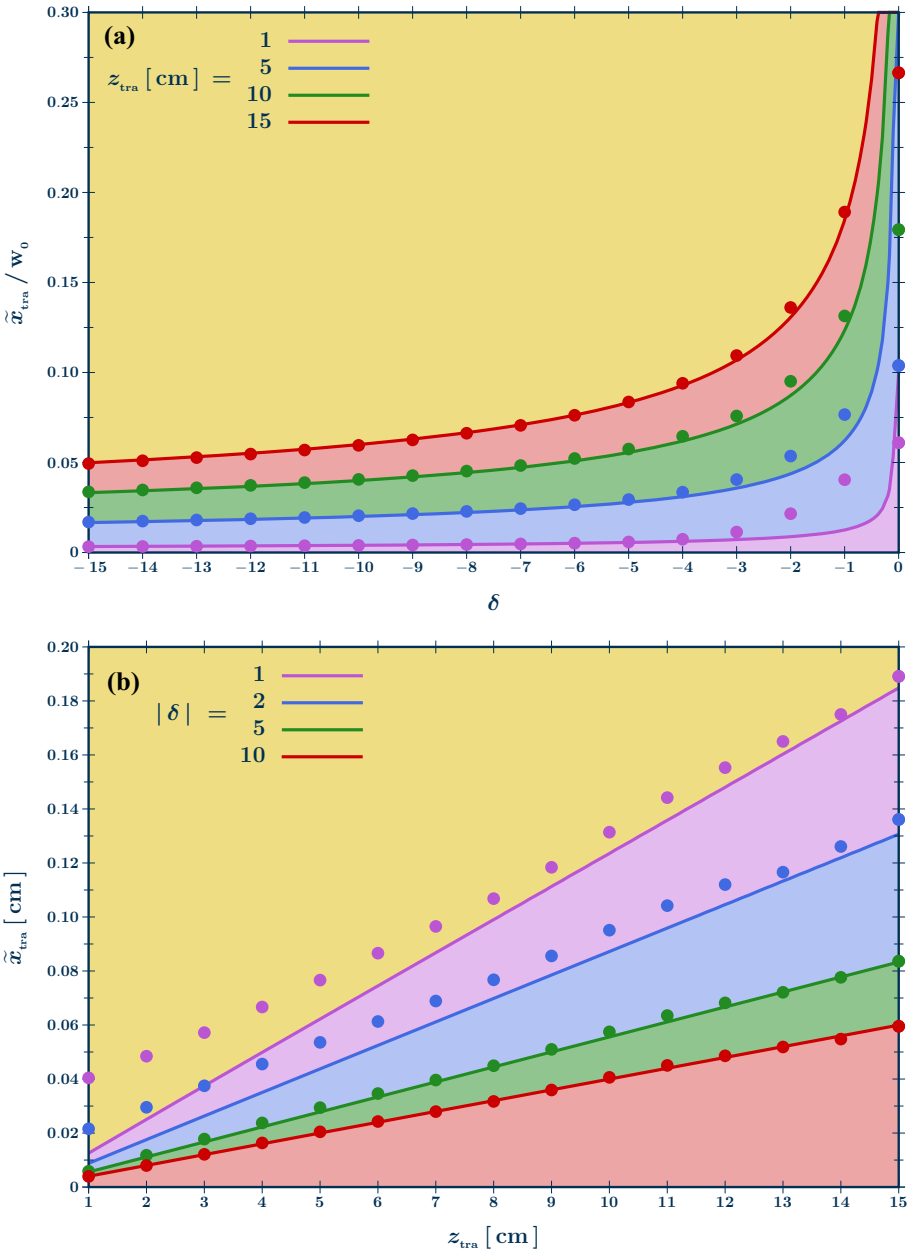

Fig. 4 Angular deviations for transverse magnetic beam (upper) transmitted through a dielectric prism for incidence approaching the critical angle. In (**a**), the shift of peak as a function of the incidence angle for different axial distances. In (**b**), the shift is plotted as a function of the axial distance for different values of the incidence angle. Analytic and numerical data show agreement for $\delta \leq -5$

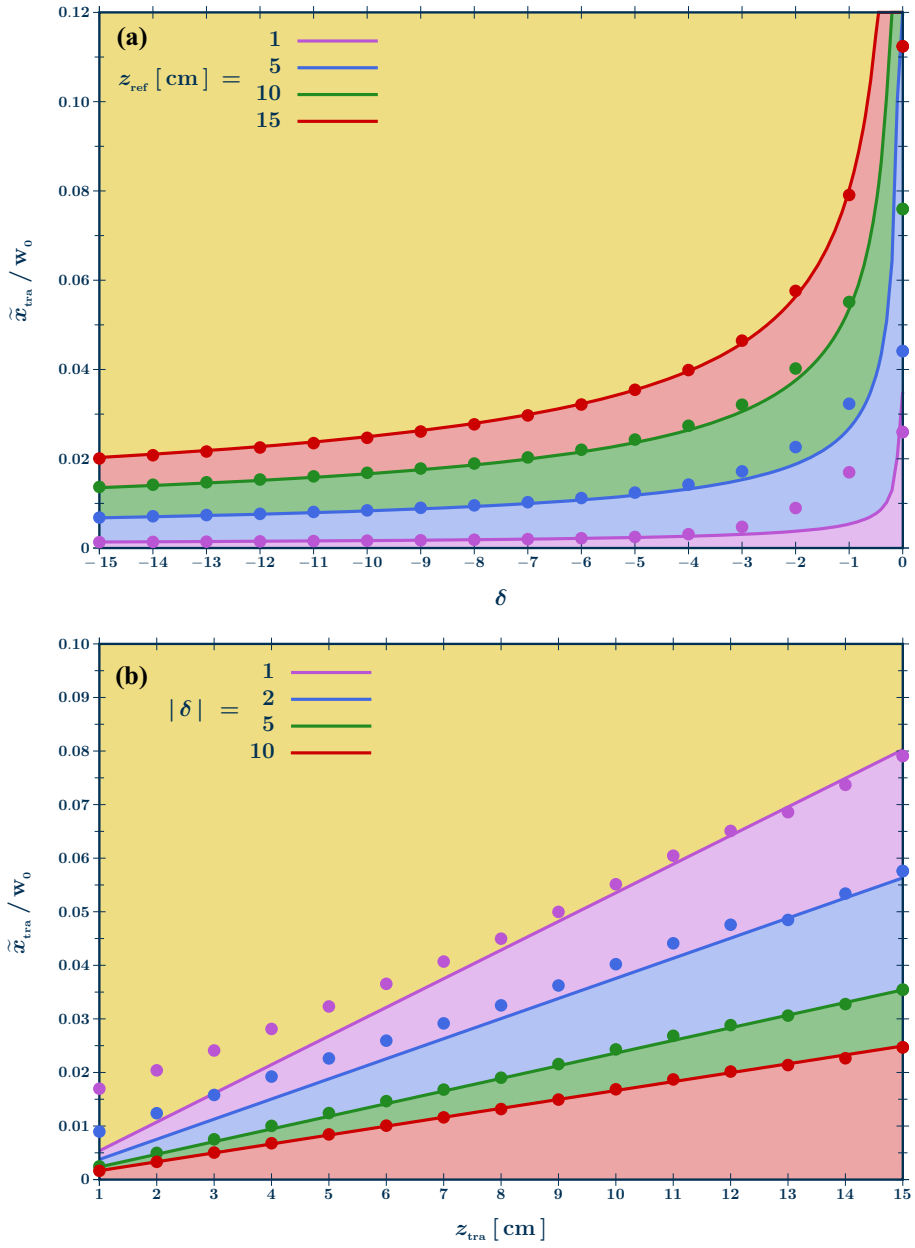

Fig. 5 The same of Fig. 4 for transverse electric beams

By using

$$\frac{\int \mathrm{d}x_{\mathrm{ref}} \int \mathrm{d}y \; x_{\mathrm{ref}}^{2} \, I^{[\mathrm{inc}]}(x_{\mathrm{ref}}, y, z_{\mathrm{ref}})}{\int \mathrm{d}x_{\mathrm{ref}} \int \mathrm{d}y \; I_{\mathrm{pol}}^{[\mathrm{ref}]}(x_{\mathrm{ref}}, y, z_{\mathrm{ref}})} = \frac{\mathrm{w}^{2}(z_{\mathrm{ref}})}{4},$$

we then obtain

$$\langle x_{\mathrm{ref}} \rangle_{\mathrm{pol}} = \frac{2\,\alpha_{\mathrm{pol}}}{(k\,\mathrm{w}_0)^2 + \alpha_{\mathrm{pol}}^2} \; z_{\mathrm{ref}}. \tag{13}$$

For transverse electric waves $k\,\mathrm{w}_0 \gg \alpha_{\mathrm{te}}$, the mean value calculation of angular deviations is proportional to $1/(k\,\mathrm{w}_0)^2$ and so very small, for the beam parameters used in this work, $k\mathrm{w}_0 \approx 1.2 \times 10^3$. For transverse magnetic waves, in the case of the incidence near the Brewster angle, $\theta_{\mathrm{exB}} + \delta\,/\,(k\,\mathrm{w}_0)$, the factor

$$\alpha_{\mathrm{tm}} \;\rightarrow\; k\,\mathrm{w}_0\,/\,\delta,$$

and it acts as an amplification

$$\langle x_{\mathrm{ref}} \rangle_{\mathrm{tm}} = \frac{2\,\delta}{\delta^2 + 1} \; \frac{z_{\mathrm{ref}}}{k\,\mathrm{w}_0}. \tag{14}$$

From Fig. 2, we see that for $\delta = 1$ (i.e. incidence at $\theta_{\mathrm{exB}} + 0.05^{o}$) the mean value, due to the presence of a secondary peak, does not coincide with the maximum of the reflected intensity. In the next Section, we shall focus our attention on the asymmetry of the reflected beam.

3.3 The cubic equation

In order to calculate the angular deviations of the peak of the reflected beam, we equalize to zero the derivative of Eq. (8). After simple algebraic manipulations, we find

$$x_{\mathrm{ref}}^{3} + a_2^{\mathrm{pol}}\, x_{\mathrm{ref}}^{2} + a_1^{\mathrm{pol}}\, x_{\mathrm{ref}} = a_0 \tag{15}$$

where

$$a_2^{\mathrm{pol}} = 2\,z_{\mathrm{ref}}\,/\,\alpha_{\mathrm{pol}},$$
$$a_1^{\mathrm{pol}} = \frac{\mathrm{w}^{2}(z_{\mathrm{ref}})}{2}\left[2\left(\frac{z_R}{\mathrm{w}_0\,\alpha_{\mathrm{pol}}}\right)^{2} - 1\right],$$

and

$$a_0^{\mathrm{pol}} = z_{\mathrm{ref}}\,\mathrm{w}^{2}(z)/\,2\,\alpha_{\mathrm{pol}}.$$

For transverse electric waves, $k\,\mathrm{w}_0 \gg \alpha_{\mathrm{te}}$ and this allows to simplify the cubic equation to a linear one

$$a_1^{\mathrm{te}}\, x_{\mathrm{ref}}^{\mathrm{te}} = a_0,$$

with $a_1^{\mathrm{te}} = [\mathrm{w}(z_{\mathrm{ref}})\,k\,\mathrm{w}_0/2\,\alpha_{\mathrm{te}}]^2$, and, consequently, to recover the mean value result $2\,\alpha_{\mathrm{te}}\,z_{\mathrm{ref}}/(k\,\mathrm{w}_0)^2$. This shows a symmetry in the reflected (transverse electric) beam.

Let us now analyse the cubic equation for transverse magnetic waves and incidence near the Brewster angle,

$$\widetilde{\theta} = \theta_{\text{exB}} + \delta / k\, \text{w}_0.$$

In this case, $\alpha_{\text{tm}} \approx k\, \text{w}_0 / \delta$ and the cubic equation becomes

$$\frac{x_{\text{ref}}^3}{\text{w}_0^3} + b_2^{\text{tm}} \frac{x_{\text{ref}}^2}{\text{w}_0^2} + b_1^{\text{tm}} \frac{x_{\text{ref}}}{\text{w}_0} = b_0^{\text{tm}}, \tag{16}$$

where

$$\{ b_2^{\text{tm}}, b_1^{\text{tm}} \} = \{ \delta\, z_{\text{ref}} / z_R, (\delta^2 - 2)\, \text{w}^2(z_{\text{ref}}) / 4\, \text{w}_0^2 \},$$

and

$$b_0^{\text{tm}} = \delta\, z_{\text{ref}}\, \text{w}^2(z_{\text{ref}}) / 4\, z_R \text{w}_0^2.$$

In Fig. 3, we draw the solutions of Eq. (16), continuous lines, as a function of δ for different values of z_{ref} (upper plots) and as a function of $z_{\text{ref}}/\text{w}_0$ for different values of δ. The dashed lines and dots, respectively, correspond to the mean value and numerical calculation. By decreasing the values of δ and z_{ref}, we amplify the effect of breaking of symmetry and, consequently, the mean value calculation does not represent a good estimate of the angular deviations. The cubic equation solutions show an excellent agreement with the numerical data.

3.4 The universal solution

In view of experimental implementations, it should be interesting to find an explicit and, possibly, universal solution of the cubic equation. As seen in Fig. 2, for incidence near the Brewster angle an additional peak appears and, in this case, the concept of angular deviations is misleading. Nevertheless, when we increase the axial distance, one of the peaks tends to disappear. This observation leads the authors to consider the limit $z_{\text{ref}} \gg z_R$ in the cubic equation (16). Under such a condition, we can use the approximation

$$\text{w}(z_{\text{ref}}) \approx \text{w}_0\, z_{\text{ref}} / z_R$$

and rewrite the coefficients of the cubic equation as follows

$$\{ \widetilde{b}_2^{\text{tm}}, \widetilde{b}_1^{\text{tm}} \} = \{ \delta\, z_{\text{ref}} / z_R, (\delta^2 - 2)\, z_{\text{ref}}^2 / 4\, z_R^2 \},$$

and

$$\widetilde{b}_0^{\text{tm}} = \delta\, z_{\text{ref}}^3 / 4\, z_R^3.$$

By substituting these coefficients in the cubic equation (16), we obtain the *universal* equation

$$4\, \rho^3 + 4\, \delta\, \rho^2 + (\delta^2 - 2)\, \rho = \delta, \tag{17}$$

where

$$\rho = \frac{z_R\, x_{\text{ref}}}{z_{\text{ref}}\, \text{w}_0}.$$

The explicit solution of Eq. (17), which is given by

$$\left\{ -\frac{\sqrt{\delta^2 + 8} + \delta}{4}, -\frac{\delta}{2}, \frac{\sqrt{\delta^2 + 8} - \delta}{4} \right\}, \tag{18}$$

contains the information on the two maxima (left and right values) and the minimum (central value). For $\delta = 0$, we recover the double peaks phenomenon with the minimum locates at the Brewster angle. For $\delta = 1$, the main peak is found at $\rho = 1/2$ and this implies

$$x_{\text{ref}} = z_{\text{ref}} / k\, \text{w}_0.$$

This means, in the case of an optical beam with $\text{w}_0 = 100\,\mu\text{m}$ and $\lambda = 532\,\text{nm}$, an angular deviation of approximatively $0.05°$ with respect to the optical path predicted by the Snell law with an amplification of a factor $k\,\text{w}_0$ ($\approx 10^3$) with respect to the angular deviations of transverse electric waves.

4 The (upper) transmitted beam

The Fresnel coefficient for the (upper) transmitted beam, $T_{\text{pol}}(k_x, k_y)$, contains the double transmission through the left (air/dielectric) and right(dielectric/air) interfaces,

$$\frac{4\, n \cos\theta\, \cos\psi}{(a_{\text{pol}} \cos\theta + n \cos\psi / a_{\text{pol}})^2},$$

the reflection at the lower (dielectric/air) interface,

$$\frac{n \cos\varphi / a_{\text{pol}} - a_{\text{pol}} \cos\phi}{n \cos\varphi / a_{\text{pol}} + a_{\text{pol}} \cos\phi},$$

and, finally, the optical phase,

$$\exp\{\, i\, [\, n\, \cos\varphi\, d\, \sqrt{2}\, +\, (\, n\, \cos\psi\, -\, \cos\theta\,)\, (\, \ell\, -\, d\,)\,]\, \},$$

which takes into account the distance between the lower and right (dielectric) interfaces and the left (air/dielectric) one. This phase is responsible for the optical path predicted by the ray optics [39].

As done for the reflected beam, we consider the first-order Taylor expansion,

$$\begin{aligned} T_{\text{pol}}(k_x, k_x) = T_{\text{pol}}(0,0) \left[1 + \beta_{\text{pol}} \frac{k_x}{k} \right] \\ \times \exp[- i\, k_x\, x_{\text{Snell}}] \end{aligned} \tag{19}$$

where

$$x_{\text{Snell}} = (\tan\psi \cos\theta - \sin\theta)\, \ell + (\cos\theta + \sin\theta)\, d,$$

and

$$\beta_{\text{pol}} = \beta_{\text{pol}}^{[1]} + \beta_{\text{pol}}^{[2]} + \beta_{\text{pol}}^{[3]},$$

with

$$\begin{aligned} \beta_{\text{te}}^{[1]} &= \tan\psi - \tan\theta, \\ \beta_{\text{te}}^{[2]} &= 2\, \tan\phi\, \cos\theta / n\, \cos\psi, \\ \beta_{\text{te}}^{[3]} &= (\tan\theta - \tan\psi)\, \cos\theta / n\, \cos\psi, \\ (\sin^2\psi - \cos^2\theta)\, \beta_{\text{tm}}^{[1]} &= \tan\psi - \tan\theta / n^2, \\ (\sin^2\phi - \cos^2\varphi)\, \beta_{\text{tm}}^{[2]} &= 2\, \tan\phi\, \cos\theta / n\, \cos\psi, \end{aligned}$$

$$(\sin^2\theta - \cos^2\psi)\,\beta_{\rm tm}^{[3]} = (\tan\theta - n^2\tan\psi)\,\cos\theta/n\,\cos\psi.$$

The first-order expansion of the Fresnel coefficient allows to analytically solve the integral equation (5),

$$E_{\rm pol}^{[\rm tra]}(x_{\rm tra}, y, z_{\rm tra}) = \left[1 + i\,\frac{\beta_{\rm pol}\widetilde{x}_{\rm tra} + z_{\rm tra}}{z_R}\right] \times \frac{T_{\rm pol}(0,0)}{1 + i\,z_{\rm tra}/z_R}\,E^{[\rm inc]}(\widetilde{x}_{\rm tra}, y, z_{\rm tra}), \tag{20}$$

where $\widetilde{x}_{\rm tra} = x_{\rm tra} - x_{\rm Snell}$.

For the (upper) transmitted beam, before calculating the intensity we have to spend some words on the $\beta_{\rm pol}^{[2]}$ coefficients. Two angles play an important role, the internal Brewster angle,

$$\sin\phi_{\rm inB} = \cos\varphi_{\rm inB} \quad \Rightarrow \quad \varphi_{\rm inB} = \arctan(1/n)\ ,$$

and the critical one

$$\cos\phi_{\rm cri} = 0 \quad \Rightarrow \quad \varphi_{\rm cri} = \arcsin(1/n).$$

When the incidence angle approaches the internal Brewster or critical region, the $\beta_{\rm tm}^{[2]}$ and $\beta_{\rm pol}^{[2]}$ coefficients act as an amplification factor of angular deviations. For

$$\theta_{\rm cri} < \frac{1 - \sqrt{n^2 - 1}}{\sqrt{2}}, \tag{21}$$

the $\beta_{\rm pol}$ coefficients are real and the (upper) transmitted intensity is then given by

$$I_{\rm pol}^{[\rm tra]}(x_{\rm tra}, y, z_{\rm tra}) = \left[1 + \left(\frac{\beta_{\rm pol}\widetilde{x}_{\rm tra} + z_{\rm tra}}{z_R}\right)^2\right] \times \frac{\mathrm{w}_0^2}{\mathrm{w}^2(z_{\rm tra})}\,T_{\rm pol}^2(0,0)\,I^{[\rm inc]}(\widetilde{x}_{\rm tra}, y, z_{\rm tra}). \tag{22}$$

In both the Brewster angle and the critical one, the coefficient $\beta^{[2]}$ tends to infinity, although for different reasons. In the following sections, the analysis of the angular deviations for these regions is provided.

4.1 The internal Brewster angle

As observed in the previous Section, the internal Brewster angle is found at $\tan\varphi_{\rm cri} = 1/n$. This implies an incidence angle of

$$\theta_{\rm inB} = \arcsin\left[\frac{n\,(1 - n)}{\sqrt{2\,(1 + n^2)}}\right]. \tag{23}$$

At such an incidence, the infinity of the $\beta_{\rm tm}^{[2]}$ coefficient is compensated by the zero in $T_{\rm tm}(0,0)$. This allows, as done for the reflected beam, to find a closed form for the (upper) transmitted intensity at the internal Brewster angle,

$$I_{\rm inB}^{[\rm tra]}(x_{\rm tra}, y, z_{\rm tra}) = \left[g(n)\,\frac{\widetilde{x}_{\rm tra}}{z_R}\,\frac{\mathrm{w}_0}{\mathrm{w}^2(z_{\rm tra})}\right]^2 \times I^{[\rm inc]}(\widetilde{x}_{\rm tra}, y, z_{\rm tra}), \tag{24}$$

where

$$
\begin{aligned}
g(n) &= \lim_{\theta \to \theta_{\text{inB}}} \beta_{\text{tm}} T_{\text{tm}}(0,0) \\
&= \frac{4\sqrt{n^2+1}}{\left(n + \dfrac{1+n}{\sqrt{2+n^2+2n^3-n^4}}\right)^2} \\
&\quad \times \lim_{\theta \to \theta_{\text{inB}}} \frac{\cos\varphi - n\cos\phi}{\sin^2\phi - \cos^2\varphi} \\
&= \frac{2(n^4-1)}{n\left(n + \dfrac{1+n}{\sqrt{2+n^2+2n^3-n^4}}\right)^2}.
\end{aligned}
$$

From Eq. (22), we obtain a cubic equation like the one obtained for the reflected beam (15). The cubic equation that now contains β_{pol} instead of α_{pol} allows to determine the peak of the upper transmitted beam and consequently the angular deviations. For incidence approaching the internal Brewster angle, $\widetilde{\theta} = \theta_{\text{inB}} + \delta / k\, \text{w}_0$, we find $\beta_{\text{tm}} \approx k\, \text{w}_0 / \delta$ and so we recover Eq. (16) and for axial distance greater than the Rayleigh range Eq. (17). Finally, the reflected and (upper) transmitted beam show the same behaviour for incidence in the Brewster region. The numerical calculation confirms our analytical results.

4.2 The critical angle

For incidence approaching the critical region, both the transverse magnetic and electric $\beta^{[2]}$ coefficient act as angular deviations amplification factors. This is due to the presence in the denominator of $\beta^{[2]}_{\text{pol}}$ of $\cos\phi$ which tends to zero when θ tends to θ_{cri}. Contrarily to what happens for the Brewster angles this zero in the denominator is not compensated by the zero in the Fresnel coefficient. This implies that, in the critical region,

$$\theta_{\text{cri}} + \delta / k\, \text{w}_0,$$

the first-order expansion of the (upper) transmitted beam (22) and, consequently, the cubic equation obtained for the angular deviation (15), with β_{pol} instead of α_{pol}, is valid for $\delta \geq 5$. For these values of δ, the main contribution to the (upper) transmitted beam comes from the real part of the Fresnel coefficient and, in this case, the first-order expansion represents a good approximation for the beam.

Figures 4 (for the transverse magnetic waves) and 5 (for the electric ones) show the angular deviations calculated by using the cubic equation (15) with β_{pol} in the a-coefficients (continuous lines), and the ones obtained by the numerical analysis (dots). For $\delta \leq -5$, the analytical curves and numerical data show an excellent agreement. The plots in Figures 4 and 5 also show an interesting result: For $\delta > -5$, the analytical curves show an agreement with the numerical data when we increase the axial distance. This phenomenon clearly deserves future investigation and could shed new light to the field expansion for incidence near the critical angle.

5 Conclusions

The first consequence of the symmetry of the wave number distribution of a free Gaussian beam is that the mean value and peak position of the optical beam coincide. Reflection by and transmission through a dielectric prism breaks this symmetry. The mathematical reason is the presence of the Fresnel coefficients in the wave number distributions of the reflected and transmitted beams. The breaking of symmetry is then responsible for angular deviations from geometric optics. In this paper, by using the first-order Taylor expansion of the Fresnel coefficients, we find an analytic expression for the intensity of the optical beam reflected by and (upper) transmitted through a dielectric prism, see Eqs. (8) and (22). The closed expressions are then verified by numerical calculations for incidence near the Brewster angle showing an excellent agreement as can be seen in Fig. 2. From these analytical formulas, we find a cubic equation which allows to determine the peak of the optical beams and to compare them with the mean value calculation. For transverse magnetic waves, when the incidence angle approaches the Brewster angle, $\delta/k\,\mathrm{w}_0$, the breaking of symmetry becomes evident and in the limit $\delta = 0$ it generates the well-known phenomenon of double peaks. In this region, for an axial distance greater than the Rayleigh range, it is also possible to find a universal solution for the main peak

$$\frac{z_R\, x_{\mathrm{peak}}}{z_{\mathrm{beam}}\, \mathrm{w}_0} = \frac{\sqrt{\delta^2 + 8} - \delta}{4}.$$

This simple and universal formula, explicitly, shows an amplification of a factor $k\,\mathrm{w}_0$ with respect to the angular deviations of transverse electric waves which are approximatively of the order of $1/(k\,\mathrm{w}_0)^2$. It is also important to observe that, notwithstanding the Fresnel coefficients depend on the refractive index, the angular deviations, in this limit, does not depend on it. In this paper, it has also been proved that reflected and (upper) transmitted beams show the same behaviour when the incidence approaches the external and internal Brewster angles. From the previous formula, we immediately see that for $\delta = 1$ (in the case analysed in this paper, $\mathrm{w}_0 = 100\,\mu$m and $\lambda = 532$ nm, this means an incidence 0.05^o around the Brewster angle) and an axial distance twice the Rayleigh range the shift of the peak with respect to the position predicted by the geometric optics is w_0. For the (upper) transmitted beam, when the incidence angle approaches the critical one, angular deviations are amplified both for transverse and for magnetic waves. The amplifications in the critical region are smaller than the ones seen in the Brewster region. Finally, angular deviations are also present in the lower transmitted beam and they represent additional effects to the laser planar trapping recently discussed in the literature [40]. This topic will be investigated in future studies.

The analytical results found in this paper could be very useful in future experimental studies. In view of possible experimental implementations, it is important to observe that two kind of experiments can be realized. A first possibility is to use an incident transverse magnetic beam and, then, to detect the reflected beam by using a camera positioned parallel to the first prism interface and by increasing its axial distance. Approaching the Brewster angle, we should find deviation from the angular prediction of the refection law. A second possibility is represented by mixing transverse electric and magnetic waves. The incidence angle is then chosen near the critical angle. The technique of weak measurements [34] allows to further amplify the angular deviations of the (upper) transmitted beam. For this technique, the closed expressions for the transverse electric and magnetic beams presented in this work

will play a fundamental role in determining the shift between the peaks of the transmitted beam.

Acknowledgements One of the authors (S.D.L.) thanks the CNPq (grant 2018/303911) and Fapesp (grant 2019/06382-9) for financial support. The authors are also grateful to A. Alessandrelli, L. Maggio, and L. Solidoro for their scientific comments and suggestions during the preparation of this article and to Profs. G. Co′, L. Girlanda, M. Martino, and M. Mazzeo for their help in consolidating the research *BRIT* project of international collaboration between the State University of Campinas (Brazil) and the Salento University of Lecce (Italy).

References

1. M. Born, E. Wolf, *Principles of optics* (Cambridge UP, Cambridge, 1999)
2. B.E.A. Saleh, M.C. Teich, *Fundamentals of Photonics* (Wiley & Sons, New Jersey, 2007)
3. F. Goos, H. Hänchen, Ein neuer und fundamentaler Versuch zur Totalreflexion. Ann. Physik **436**, 333–346 (1947)
4. K. Artmann, Berechnung der Seitenversetzung des totalreflektierten Strahles. Ann. Physik **437**, 87–102 (1948)
5. C. Fragstein, Zur Seitenversetzung des totalreflektierten Lichtstrahles. Ann. Physik **439**, 217–278 (1949)
6. F. Goos, H. Lindberg-Hänchen, Neumessung des Strahlwersetzungseffektes bei Totalreflexion. Ann. Physik **440**, 251–252 (1949)
7. K. Artmann, Beugung an einer einbackigen Blende endlicher Dicke and der Zusammenhang mit der Theorie der Seitenversetzung des totalref lektierten Strahles. Ann. Physik **442**, 209–212 (1950)
8. R.H. Renard, Total reflection: a new evaluation of the Goos-Hänchen shift. JOSA **54**, 1190–1197 (1964)
9. H.K.V. Lotsch, Reflection and refraction of a beam of light at a plane interface. JOSA **58**, 551–561 (1968)
10. B.R. Horowitz, T. Tamir, Lateral displacement of a light beam at a dielectric interface. JOSA **61**, 586–594 (1971)
11. J.L. Carter, H. Hora, Total reflection of matter waves: The Goos-Haenchen effect for grazing incidence. JOSA **61**, 1640–1645 (1971)
12. J.J. Cowan, B. Anicin, Longitudinal and transverse displacements of a bounded microwave beam at total internal reflection. JOSA **67**, 1307–1314 (1977)
13. F. Bretenaker, A. Le Floch, L. Dutriaux, Direct measurement of the optical goos-Hänchen effect in lasers. Phys. Rev. Lett. **68**, 931–933 (1992)
14. A. Aiello, J.P. Woerdman, Role of beam propagation in Goos-Hänchen and Imbert-Fedorov shifts. Opt. Lett. **33**, 1437–1439 (2008)
15. A. Aiello, Goos-Hänchen and Imbert-Fedorov shifts: a novel perspective. New J. Phys. **14**, 013058–12 (2012)
16. K.Y. Bliokh, A. Aiello, Goos-Hänchen and Imbert-Fedorov beam shifts: an overview. J. Opt. **15**, 014001–16 (2013)
17. G. Jayaswal, G. Mistura, M. Merano, Weak measurement of the Goos-Hänchen shift. Opt. Lett. **38**, 1232–1234 (2013)
18. L.G. Wang, S.Y. Zhu, M.S. Zubairy, Goos-Hänchen shifts of partially coherent light fields. Phys. Rev. Lett. **111**, 223901–5 (2013)
19. M.P. Araújo, S.A. Carvalho, S. De Leo, The frequency crossover for the Goos-Hänchen shift. J. Mod. Opt. **60**, 1772–1780 (2013)
20. M.P. Araújo, S. De Leo, G.G. Maia, Closed form expression for the Goos-Hänchen lateral displacement. Phys. Rev. A **93**, 023801–023809 (2016)
21. O. Santana, S.A. Carvalho, S. De Leo, L.E.E. de Araujo, Weak measurement of the composite Goos-Haenchen shift in the critical region. Opt. Lett. **41**, 3884–3887 (2016)
22. V. Kompanets, A. Melnikov, S. Chekalin, Goos-Hänchen shift of a mid-infrared femtosecond filament visualized by the laser coloration method. Las. Phys. Lett. **18**, 015302–5 (2021)
23. Y.M. Antar, W.M. Boerner, Gaussian beam interaction with a planar dielectric interface. Can. J. Phys. **52**, 962–972 (1974)
24. I.A. White, A.W. Snyder, C. Pask, Directional change of beams undergoing partial reflection. JOSA **67**, 703–705 (1977)
25. C.C. Chan, T. Tamir, Angular shift of a Gaussian beam reflected near the Brewster angle. Opt. Lett. **10**, 378–380 (1985)

26. C.C. Chan, T. Tamir, Beam phenomena at and near critical incidence upon a dielectric interface. JOSA A **4**, 665–663 (1987)
27. D. Müller, D. Tharanga, A.A. Stahlhofen, G. Nimtz, Nonspecular shifts of microwaves in partial reflection. Europhys. Lett. **73**, 526–532 (2006)
28. A. Aiello, J. P. Woerdman, Theory of angular Goos-Hänchen shift near Brewster incidence. arXiv:0903.3730 [physics.optics] (2009)
29. A. Aiello, M. Merano, J.P. Woerdman, Brewster cross polarization. Opt. Lett. **34**, 1207–1209 (2009)
30. M. Merano, A. Aiello, M.P. Exter, J.P. Woerdman, Observing angular deviations in the specular reflection of a light beam. Nat. Photonics **3**, 337–340 (2009)
31. M. Merano, N. Hermosa, J.P. Woerdman, A. Aiello, How orbital angular momentum affects beam shifts in optical reflection. Phys. Rev. A **82**, 023817–5 (2010)
32. J.B. Götte, S. Shinohara, M. Hentschel, Are Fresnel filtering and the angular Goos-Hänchen shift the same? J. Opt. **15**, 014009–041008 (2013)
33. M.P. Araújo, S.A. Carvalho, S. De Leo, Maximal symmetry breaking at critical angle and closed form expression for angular deviations of the Snell law. Phys. Rev. A **90**, 033844–033851 (2014)
34. M.P. Araújo, S. De Leo, G.G. Maia, Optimizing weak measurements to detect angular deviations. Ann. Physik **529**, 1600357–20 (2017)
35. S. De Leo, G.G. Maia, Lateral shifts and angular deviations of Gaussian optical beams reflected by and transmitted through dielectric blocks: a tutorial review. J. Mod. Opt. **66**, 2142–2194 (2019)
36. M.P. Araújo, S. De Leo, G.G. Maia, Oscillatory behavior of light in the composite Goos-Hänchen shift. Phys. Rev. A **95**, 053836–053839 (2017)
37. O. Santana, L.E.E. de Araujo, Direct measurement of the composite Goos-Hänchen shift of an optical beam. Opt. Lett. **43**, 4037–4040 (2018)
38. O. Santana, L.E.E. de Araujo, Oscillatory trajectory of an optical beam propagating in free space. Opt. Lett. **44**, 646–649 (2019)
39. S.A. Carvalho, S. De Leo, The use of the stationary phase method as a mathematical tool to determine the path of optical beams. Am. J. Phys. **83**, 249–255 (2015)
40. S. De Leo, Laser planar trapping. Las. Phys. Lett. **17**, 116001–10 (2020)